Jurnal Penelitian Fisika dan Aplikasinya (JPFA)
Volume 12, Issue 2, December 2022
https://journal.unesa.ac.id/index.php/jpfa/

p-ISSN: 2087-9946
e-ISSN: 2477-1775

Severity Classification of Non-Proliferative Diabetic Retinopathy Using Support Vector Machine (SVM)

Siti Salamah [a,*], Khoerun Nisa Syaja'ah [b], and Yudha Satya Perkasa [c]

Department of Physics, Faculty of Science and Technology, Universitas Islam Negeri Sunan Gunung Djati
Jalan A.H Nasution No. 105 Cibiru, Bandung 40615, Indonesia

e-mail: [a] salamahsiti1310@gmail.com, [b] nisasya@uinsgd.ac.id, and [c] yudha@uinsgd.ac.id
* Corresponding Author

Received: 15 October 2022; Revised: 30 November 2022; Accepted: 30 December 2022

Abstract

Diabetic Retinopathy (DR) is an eye disease that is the main cause of blindness in developed countries. Treatment of DR and prevention of blindness depend heavily on regular monitoring, early-stage diagnosis, and timely treatment. Vision loss can be effectively prevented by the automated diagnostic system that assists ophthalmologists who otherwise practice manual lesion detection processes which are tedious and time-consuming. Therefore, the purpose of this research is to design a system that can detect the presence of DR and be able to classify it based on its severity. In this proposed, the classification process is carried out based on image discovery by extracting GLCM texture features from 454 retinal fundus images in the IDRiD database which are classified into 4 severity levels, namely normal, mild NPDR, moderate NPDR, and severe NPDR. The features obtained from each image are used as input for the classification process using SVM. As a result, the classification system that has been trained is able to classify 4 levels of DR severity with an average accuracy of 89.55%, a sensitivity of 81.03%, and a specificity of 92.89%. Based on the results of the evaluation of the performance of this classification system, it can be concluded that the specificity value is higher than the sensitivity value, this indicates that the system that has been trained has a good ability to identify negative samples or those that indicate a class.

Keywords: *Retinal Fundus Image; GLCM Feature Extraction; Diabetic Retinopathy; Segmentation; Support Vector Machine*

How to cite: Salamah S, et al. Severity Classification of Non-Proliferative Diabetic Retinopathy Using Support Vector Machine (SVM). *Jurnal Penelitian Fisika dan Aplikasinya (JPFA)*. 2022; **12**(2): 167-179.

INTRODUCTION

Diabetic Retinopathy (DR) is an eye disease that posits as the main cause of blindness in developed countries [1] due to complications of diabetes mellitus (DM) [2]. The number of DM patients is increasing every year. In 2017, DM patients in the world reached 425 million and it is

DOI: 10.26740/jpfa.v12n2.p167-179

estimated that in 2045 it will reach 629 million [3]. The increasing number of DM patients will also be at risk of an increase in DR. Therefore, DM patients require regular retinal screening to detect DR early and avoid the risk of blindness [4].

DR can be detected effectively with an automated diagnostic system that assists ophthalmologists in practicing the tedious and time-consuming process of manual lesion detection [5]. Computer-aided diagnosis (CAD) may hold the key to the problem. Computer-aided screening systems have recently gained importance for increasing the feasibility of DR screening, and several algorithms have been developed for the automated detection of lesions such as exudates (EX), hemorrhages (HM), and microaneurysms (MA) [6].

Several previous works have reported the automatic detection of DR using several machine-learning techniques. Some of these methods are the Support Vector Machine (SVM) method [7–10], the K-Nearest Neighbor (KNN) method [7,11,12], the Random Forest (RF) method [7,13–16], Decision Tree (DT) method [7,17], Artificial Neural Network (ANN) method [18,19], and Probabilistic Neural Network (PNN) method [9].

However, in their article, Alyoubi [4], mentions that research on the classification of the severity of DR is still very rare. In most of the studies, almost 73% only classify fundus images using binary classifications such as DR or normal, while it was only found that only 27% classified DR based on its severity. Meanwhile, proper identification of the severity of DR is very important in selecting the appropriate treatment process and preventing retinal damage [8].

This article focuses on the development of a diabetic retinopathy severity classification system that can detect the presence of DR as well as classify DR severity from 0 to 3. Therefore, this study aims to develop a classification system by extracting and reviewing textural features on retinal fundus images and conducting testing as well as evaluation of the performance of the classification system. So, we get a system that can detect and classify the type of severity of retinopathy automatically.

METHOD

The proposed system is implemented using Python 3.7.9 on a computer system equipped with a dual-core 2.3 GHz AMD A4-9125 APU processor and 4GB RAM. The proposed method in the DR severity assessment process is depicted in Figure 1. The proposed system consists of three main stages, namely DR lesion segmentation, GLCM feature extraction, and DR severity classification using SVM. Segmentation of DR lesions identified candidates for exudate, haemorrhage, and microaneurysms. The second stage performs GLCM feature extraction to determine the texture characteristics of the image. The third stage classifies the image into different levels according to the guidelines provided by the ICDR standard.

Dataset

This study uses a dataset sourced from the Indian Diabetic Retinopathy Image Dataset (IDRiD) repository obtained from the Eye Clinic located in Nanded, (M.S.), India. Images with symptoms of NPDR severity consist of 454 fundus images [20]. The determination of the severity of DR based on the International Clinical Diabetic Retinopathy (ICDR) is provided in Table 1. Classification of the severity stage of DR was performed using system developed by International Clinical Diabetic Retinopathy[21]. This information on determining the severity of DR is very important for deciding on follow-up treatment [20].

Table 1. Classification of the severity stage of DR was performed using system developed by International Clinical Diabetic Retinopathy

Severity Scale	Diabetic Retinopathy Grade	Description
0	Non-DR	No abnormalities
1	Mild NPDR	Microaneurysm only
2	Moderate NPDR	More number of microaneurysms but less than severe NPDR
3	Severe NPDR	More that 20 intra-retinal microaneurysms or haemorrhages
4	PDR	Neovascularization

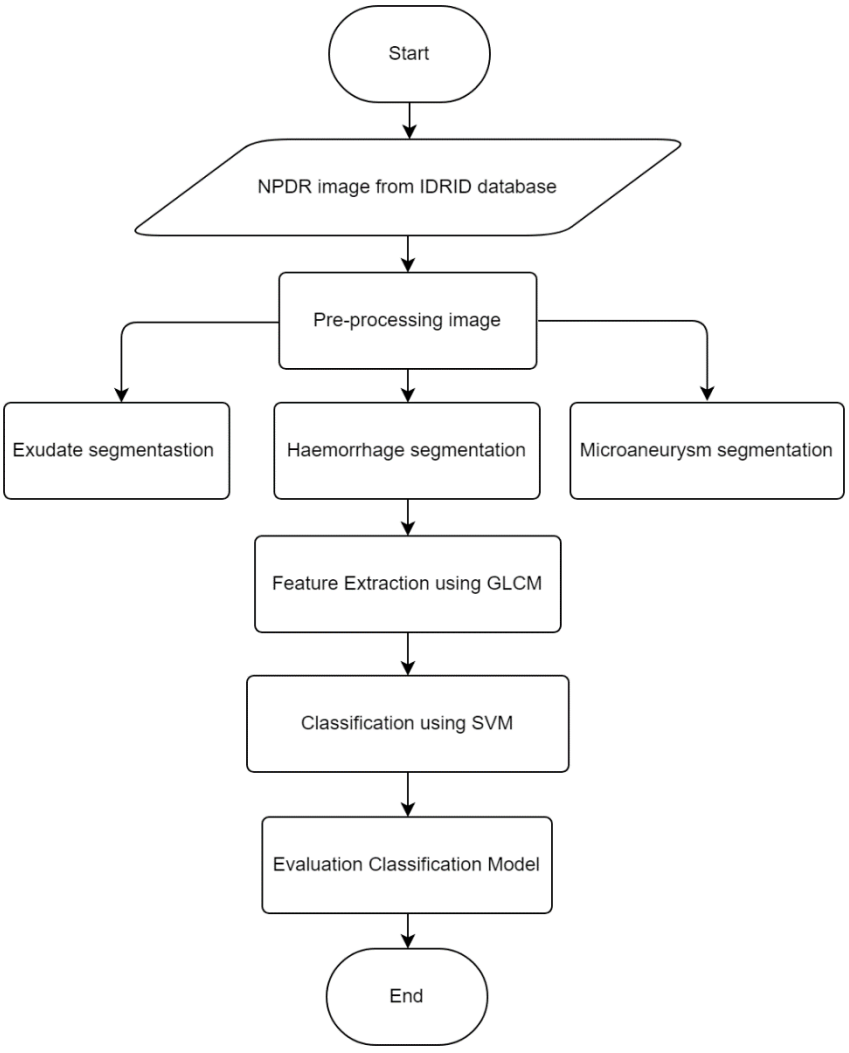

Figure 2. Framework of the proposed system

Segmentation

The segmentation process includes image preprocessing and selecting the Region of Interest (ROI) area by removing the optic disc (OD) and fovea. Preprocessing in image segmentation is to resize dimensions into smaller pixels. In addition, green channel conversion is performed on each image because the green channel has the best background so it has an optimal information

[22]. Here, the OD and fovea have similar intensity values to exudate and haemorrhage, so the OD and fovea can be removed [9]. The OD and fovea are detected by applying the Hough transformation circle equation [18] which is shown in Equation (1).

$$(x - x_c)^2 + (y - y_c)^2 + r^2 = 0 \quad (1)$$

The segmentation process is related to image processing. Some of the image processing techniques applied in this article are contrast enhancement, noise filtering, and morphological operations. The contrast enhancement process using the Contrast Limited Adaptive Histogram Equalization (CLAHE) [23]. CLAHE can solve the problem of increasing contrast that is too over, namely by giving the boundary value on the histogram. This limit value is called the clip limit which states the maximum height of a histogram [24]. Equation (2) defines the way to calculate the clip limit of a histogram.

$$\beta = \frac{M}{N}\left(1 + \frac{\alpha}{100}(s_{max} - 1)\right) \quad (2)$$

The variable M is the region size, N is the gray intensity value (256), and α is the clip boundary between 0 and 100 [24]. Median filtering is also used to remove noise from an image [25]. An example of a kernel type is the 5×5 kernel shown in Equation (3).

$$K = \frac{1}{25}\begin{bmatrix} 1 & 1 & 1 & 1 & 1 \\ 1 & 1 & 1 & 1 & 1 \\ 1 & 1 & 1 & 1 & 1 \\ 1 & 1 & 1 & 1 & 1 \\ 1 & 1 & 1 & 1 & 1 \end{bmatrix} \quad (3)$$

Morphological operations on an image are used to improve the shape of objects in order to produce more accurate features [26]. The processes of morphological operations are opening, closing, and top hat operations. The opening operation erodes an image and then dilates the eroded image, using the same structuring element for both operations, the opening process is shown in Equation (4) [27]. The closing operation dilates an image and then erodes the eroded image, the closing process is shown in Equation (5) [28]. While the top hat operation is the difference between the original input image and the opening, the top hat process is shown in Equation (6) [29].

$$A \bullet B = (A \oplus B) \ominus B \quad (4)$$

$$A \circ B = (A \ominus B) \oplus B \quad (5)$$

$$That = A - (A \bullet B) \quad (6)$$

Feature Extraction

Gray level co-occurrence matrix (GLCM) represents the relationship between two neighboring pixels that have gray intensity, distance, and angle. GLCM with size $N_g \times N_g$ is defined as $P(i, j|\delta\alpha)$ [30]. The (i, j) element of this matrix shows the combination of levels i and j that occur or appear in two image pixels [31]. The feature value is calculated from the average of the GLCM matrix for each corner. Some features extracted with GLCM [30] :

$$Contrast = \sum_{i=1}^{N_g}\sum_{j=1}^{N_g} p(i,j)(i-j)^2 \quad (7)$$

$$Entropy = \sum_{i=1}^{N_g}\sum_{j=1}^{N_g} \ln p(i,j)p(i,j) \quad (8)$$

$$Homogeneity = \sum_{i=1}^{N_g}\sum_{j=1}^{N_g} \frac{P(i,j)}{1+(i-j)^2} \quad (9)$$

where $p(i,j)$ is a normalized co-occurrence matrix $\frac{P(i,j)}{\sum P(i,j)}$

Classification

SVM works by separating hyperplanes using labeled training data and categorizing test data optimally [32]. So, the hyperplane can be represented as a set of points that satisfy Equation (10).

$$\vec{w} \cdot \vec{x} - b = 0 \tag{10}$$

where w is the normal to the hyperplane and b is the position of the plane to the center of the coordinates. The hyperplane representation for the multi-class classification problem is shown in Figure 2. SVM hyperplane that separates data between classes**.**

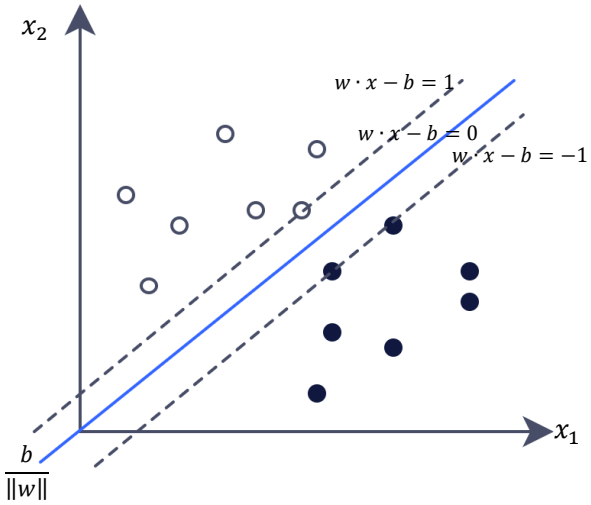

Figure 2. SVM hyperplane that separates data between classes

For multi-class DR classification problems, hypertuning parameters is employed to find the best parameters in order to achieve better accuracy for non-linear classification. Parameter optimization to avoid misclassification and gamma determines the effect of each example in the classification process [33]. The cost function for SVM classification is expressed by Equation (11).

$$\min \tau(w) = \frac{1}{2}\|w\|^2 + C \sum_{i=1}^{n} \xi_i \tag{11}$$

where ξ_i is a slack variable or also known as a soft margin hyperplane, the symbol C indicates the level of penalty (cost) for errors. The penalty rate C will affect the slack variable ξ_i [32]. SVM classification depends on kernel selection because there are different SVM kernels such as linear, polynomial, and radial basis functions (RBF) [34].

Matrix Performance

Evaluating classification performance is important to find out how well the classification performs using numerical metrics such as accuracy, sensitivity, and specificity [35]. Classification accuracy is calculated from the values of True Positive (TP), False Positive (FP), True Negative (TN), and False Negative (FN). TP is positive data that is predicted to be correct. TN is negative data that is predicted to be correct. FP is negative data but is predicted as positive data. Meanwhile, FN is positive data but is predicted as negative data. So that based on the values of TN, FP, FN, and TP, the accuracy, sensitivity, and specificity values can be obtained as calculated in Equation (12-14) [6].

$$Accuracy = \frac{TP+TN}{TP+FP+FN+TN} \tag{12}$$

$$Sensitivity = \frac{TP}{TP+FN} \tag{13}$$

$$Specificity = \frac{TN}{FP+TN} \quad (14)$$

RESULTS AND DISCUSSION

The images were segmented to see candidate lesions of MA, EX, and HM combined after the identification of pathology to classify images based on the severity of DR. GLCM features were extracted for lesion candidates at grade 1, grade 2, grade 3, and non-lesional candidates for grade 0. The extracted features were used for the classification system learning process. Furthermore, the performance of the proposed classification system is analyzed in a confusion matrix to see whether or not the system is doing the classification correctly.

Feature Extraction Result

A total of 13 features have been extracted which include ASM, contrast, correlation, variance, IDM, sum average, sum, variance, sum entropy, entropy, difference variance, difference entropy, IMC1, and IMC2 [34]. Therefore, textural directionality is a basic feature of the image and plays an important role in image descriptions, which can be used to describe image textures [13]. Table 2 provides an overview of several feature values that have been extracted from the GLCM feature class on each different label. The image storage location and image label are used as input in this process. The results of feature extraction are stored in a batch of image datasets in CSV format which are then used as inputs for the classifier process.

Table 2. Image feature extraction results with the GLCM method

Feature image	Grade 0	Grade 1	Grade 2	Grade 3
ASM	1	0.995179	0.994725	0.956563
Contrast	0	10.998438	17.186797	137.8993
Correlation	1	0.6231319	0.825809	0.883188
Variance	0	14.58897	43.34444	590.3374
IDM	1	0.998357	0.998332	0.987032
Sum average	0	0.130003	0.3941846	4.732333
Sum variance	0	47.35747	180.19096	2223.4503
Sum entropy	0	0.033852	0.0365439	0.239886
Entropy	0	0.0375971	0.0405125	0.270834
Difference variance	0	0.0038743	0.0038739	0.003599
Difference entropy	0	0.0288254	0.028272	0.1704525
IMC1	0	-0.351075	-0.453534	-0.476715
IMC2	0	0.123289	0.151599	0.390812

Training and Testing the Classification Model

A feature set of 13 GLCM features is used as input for DR severity classification [36]. After feature extraction, all features of the image will be randomly divided into training, validation, and test sets [37] with a composition of 60%: 20%: 20% respectively by considering 272 images

for the training set, 91 images for the validation set, and 91 images for the test set.

The training set will be used to train the model so that the model can see and learn from this data. The validation set is used to select a set of hyperparameters so that machine learning performance can be optimized [37]. In this study, hyperparameter tuning was performed using the GridsearchCV method on the Scikit-Learn module in Python. GridsearchCV works by trying to train every combination of parameters from the hyperparameter space in the learning algorithm so that the SVM parameter tuning results are ready for the data training process [38].

Table 3. Parameter optimization validation results on SVM

SVM parameters	Best parameters	Accuracy
'kernel': ['rbf', 'linear'],	'kernel': 'linear'	
'C': [30, 50, 100,1000],	'C': 30	93.01%
'gamma': ['scale', 'auto', 1, 0.1, 0.01,0.001]	'gamma': 'scale'	

Table 3 is the result of the validation of the parameter optimization performed on the SVM. Combinations of models and hyperparameters will be selected and tested one by one to check which combinations have good performance results. The best parameter combination is the linear kernel, with a cost value of 30, and the gamma scale. So that this parameter has a good performance in differentiating the severity label [39].

From the average optimization performance, this parameter has a good performance in differentiating severity labels. Furthermore, the system with each of these best parameters is used for testing the classification system. So, it will be given a number of test dataset features from the testing set to test its predictive ability on new data. This testing data set should never be seen by the previous model**.** Table 4 shows the results of the classification performance of the three types of sub datasets.

The training set is used to build the model using the extracted texture features [40]. In a training set, the accuracy is 96.7%. This value is good enough and the system can learn well from the data. Furthermore, a validation set is carried out to test the existing model. This aims to get feedback from the input, process, and output used [41]. Meanwhile, set testing is carried out to apply the alert model to make new data predictions [42]. Set testing also obtained very good accuracy, which was 89.55%. This means that the system can predict well from the given test dataset.

Table 4. The results of the classification performance of the three types sub datasets

Sub datasets	Accuracy
Set training	96.7%
Set validation	95.05%
Set testing	89.55%

Performance Evaluation for Classification Model

The results of the performance evaluation for the classification model using SVM are shown in Figure 3. Classification is carried out at four grades, namely level 0 as a normal image, and grades 1,2, and 3 as images with NPDR symptoms. Based on the confusion matrix in Figure 3. Evaluation of classification performance using SVM, in predicting levels 0 and 1, the system

successfully predicts all training data correctly.

Grades 2 and 3 have less than optimal results. Grade 2 is sometimes predicted by the system as grade 1. Grade 3 is also sometimes predicted as grade 2. This is reasonable because based on the determination of severity by ICDR, grades 2 and 3 have the same lesion state, namely the presence of exudate and haemorrhage, and the difference is the number of lesions. While grade 3 also has other characteristics, namely the presence of Intraretinal Microvascular Abnormalities (IRMA) which is not present in grade 2, this IRMA was not detected in the research process. This means that grade 2 has the possibility of being predicted as grade 3 because the weakness of this grade 3 IRMA is not detected.

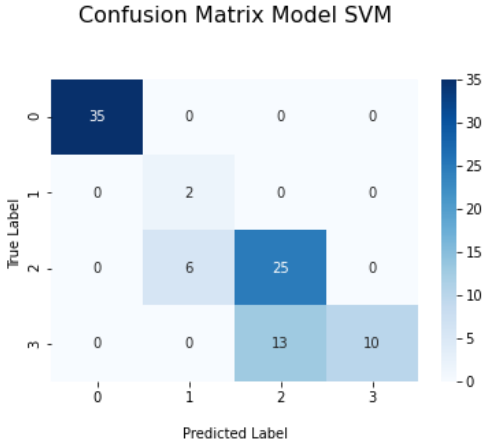

Figure 3. Evaluation of classification performance using SVM

In addition, the classification system has the accuracy, sensitivity, and specificity shown in Table 5**.** The results show a higher specificity than sensitivity. Both of these systems mean that they have a better ability to identify negative samples or those that do not indicate a class [43].

Table 5. Evaluation of classification performance

Matrix	Rate on severity				Average
	0	1	2	3	
TP	35	2	25	10	-
TN	50	83	47	68	-
FP	0	6	13	0	-
FN	0	0	6	13	-
Accuracy	100%	93.4%	79.12%	85.71%	89.55%
Sensitivity	100%	100%	80.64%	43.48%	81.03%
Specificity	100%	93.26%	78.33%	100%	92.89%

A comparative analysis of the classification system for the assessment of DR severity with 4 severity levels is shown in Table 6. The results of the comparative study show that our system provides an average accuracy of 89.55% using the SVM classifier. The comparison shows that the proposed method has a better performance in terms of accuracy than the previous studies provided.

Table 6. Comparison table for DR severity grading DR images

	Accuracy (%)

Roychowdhury et al. [6]	78.12
Seoud et al. [44]	74.10
Bhardwaj et al. [5]	91.90
This research	89.55

Based on the results and discussion, this study has several limitations, namely levels 2 and 3 have less than optimal results. This is reasonable because based on determining the level of severity with ICDR, grades 2 and 3 have the same lesion state and the difference is the number of lesions. While level 3 also has other characteristics, namely the presence of Intraretinal Microvascular Abnormalities (IRMA) which are not present at level 2, this IRMA was not detected in the research process. For further research, the authors suggest that researchers get IRMA detection procedures to obtain optimal classification results.

The results of this study are expected to be of benefit which theoretically can be used as a reference regarding a classification system for the severity of diabetic retinopathy by utilizing information from texture features extracted from an image so as to produce a system that can detect the presence of a disease automatically. Practically it can also be used as an option for a new approach to determine the severity of diabetic retinopathy as an initial clinical stage for ophthalmologists and physicians.

CONCLUSION

Based on the results obtained from this study, it is concluded that the use of GLCM texture extraction features can be used as input to the classification system. The classification system has been able to classify the severity level from level 0 to 3. Testing and evaluation of the classification system are also carried out using the lightness matrix to predict the severity of diabetic retinopathy by the classification system that has made it possible. The development of the proposed method can be extended further by focusing on the treatment of neovascularization and bleeding vascular problems that cause proliferative DR which can lead to acute blindness.

AUTHOR CONTRIBUTIONS

Siti Salamah: Conceptualization, Methodology, Software, Validation, Resources, and Writing - Original Draft; Khoerun Nisa Syajaah: Conceptualization, Methodology, Resources, Validation, and Project Administration; and Yudha Satya Perkasa: Conceptualization, Validation, and Formal Analysis.

DECLARATION OF COMPETING INTEREST

The authors declare that they have no known competing financial interests or personal relationships that could have appeared to influence the work reported in this paper.

REFERENCES

[1] Kanungo YS, Srinivasan B, and Choudhary S. Detecting Diabetic Retinopathy Using Deep Learning. *RTEICT 2017 - 2nd IEEE International Conference on Recent Trends in Electronics, Information and Communication Technology (RTEICT)*. Bangalore, India; 2017: 801–804. DOI: https://doi.org/10.1109/RTEICT.2017.8256708.

[2] Abdelsalam MM and Zahran MA. A Novel Approach of Diabetic Retinopathy Early Detection Based on Multifractal Geometry Analysis for OCTA Macular Images Using Support Vector Machine. *IEEE Access*. 2021; **9**: 22844–22858. DOI: https://doi.org/10.1109/ACCESS.2021.3054743.

[3] Handayani OWK, Nugroho E, and Hermawati B. Determinant of Diabetes Mellitus Focusing on Differences of Indonesian Culture: Case Studies in the Java and Outer Java Region in Indonesia. *The Open Public Health Journal*. 2020; **13**(1): 323–340. DOI: https://doi.org/10.2174/1874944502013010323.

[4] Alyoubi WL, Abulkhair MF, and Shalash WM. Diabetic Retinopathy Fundus Image Classification and Lesions Localization System Using Deep Learning. *Sensors*. 2021; **21**(11): 1–22. DOI: https://doi.org/10.3390/s21113704.

[5] Bhardwaj C, Jain S, and Sood M. Hierarchical Severity Grade Classification of Non-Proliferative Diabetic Retinopathy. *Journal of Ambient Intelligence and Humanized Computing*. 2021; **12**(2): 2649–2670. DOI: https://doi.org/10.1007/s12652-020-02426-9.

[6] Roychowdhury S, Koozekanani DD, and Parhi KK. DREAM: Diabetic Retinopathy Analysis Using Machine Learning. *IEEE Journal of Biomedical and Health Informatics*. 2014; **18**(5): 1717–1728. DOI: https://doi.org/10.1109/JBHI.2013.2294635.

[7] Yadav D, et al. Microaneurysm Detection Using Color Locus Detection Method. *Measurement: Journal of the International Measurement Confederation*. 2021; **176**: 109084. DOI: https://doi.org/10.1016/j.measurement.2021.109084.

[8] Amiruddin R, Stang, Ansar J, Sidik D, and Rahman AW. Diabetic Mellitus Type 2 in Wajo South Sulawesi, Indonesia. *International Journal of Current Research & Academic Review*. 2014; **2**(12): 1–8. Available from: http://www.ijcrar.com/vol-2-12/Ridwan%20Amiruddin,%20et%20al.pdf.

[9] Mahendran G and Dhanasekaran R. Investigation of the Severity Level of Diabetic Retinopathy Using Supervised Classifier Algorithms. *Computers and Electrical Engineering*. 2015; **45**: 312–323. DOI: https://doi.org/10.1016/j.compeleceng.2015.01.013.

[10] Hemavathi S and Padmapriya S. Detection of Diabetic Retinopathy on Retinal Images Using Support Vector Machine. *SSRG International Journal of Computer Science and Engineering (SSRG–IJCSE)*. 2019: **2019**(special issue ICMR); 5–8. Available from: https://www.internationaljournalssrg.org/uploads/specialissuepdf/ICMR-2019/2019/CSE/IJCSE-ICMR-P102.pdf.

[11] Koh JEW, Ng EYK, Bhandary SV, Laude A, and Acharya UR. Automated Detection of Retinal Health Using PHOG and SURF Features Extracted from Fundus Images. *Applied Intelligence*. 2018; **48**(5): 1379–1393. DOI: https://doi.org/10.1007/s10489-017-1048-3.

[12] Fayiza KT and Jabbar S. Red Lesion Detection Using Hough Transform and KNN Classifier for Diabetic Retinopathy Screening. *International Journal of Science and Research (IJSR)*. 2017; **6**(7): 473–478. DOI: https://doi.org/10.21275/art20174218.

[13] Zhang X, Cui J, Wang W, and Lin C. A Study for Texture Feature Extraction of High-Resolution Satellite Images Based on a Direction Measure and Gray Level Co-Occurrence Matrix Fusion Algorithm. *Sensors*. 2017; **17**(7): 1474. DOI: https://doi.org/10.3390/s17071474.

[14] Wang H, et al. Hard Exudate Detection Based on Deep Model Learned Information and Multi-Feature Joint Representation for Diabetic Retinopathy Screening. *Computer Methods and Programs in Biomedicine*. 2020; **191**: 105398. DOI:

https://doi.org/10.1016/j.cmpb.2020.105398.

[15] Orlando JI, Prokofyeva E, del Fresno M, and Blaschko MB. An Ensemble Deep Learning Based Approach for Red Lesion Detection in Fundus Images. *Computer Methods and Programs in Biomedicine*. 2018; **153**: 115–127. DOI: https://doi.org/10.1016/j.cmpb.2017.10.017.

[16] Liu Q, et al. A Location-to-Segmentation Strategy for Automatic Exudate Segmentation in Colour Retinal Fundus Images. *Computerized Medical Imaging and Graphics*. 2017; **55**: 78–86. DOI: https://doi.org/10.1016/j.compmedimag.2016.09.001.

[17] Aziza EZ, El Amine LM, Mohamed M, and Abdelhafid B. Decision Tree CART Algorithm for Diabetic Retinopathy Classification. *Proceedings - 2019 6th International Conference on Image and Signal Processing and their Applications, ISPA 2019*. 2019: 1–5. DOI: https://doi.org/10.1109/ISPA48434.2019.8966905.

[18] Paing MP, Choomchuay S, and Yodprom MDR. Detection of Lesions and Classification of Diabetic Retinopathy Using Fundus Images. *2016 9th Biomedical Engineering International Conference (BMEiCON)*. Laung Prabang, Laos; 2016: 1-5. DOI: https://doi.org/10.1109/BMEiCON.2016.7859642.

[19] Nayak J, Bhat PS, Acharya R, Lim CM, and Kagathi M. Automated Identification of Diabetic Retinopathy Stages Using Digital Fundus Images. *Journal of Medical Systems*. 2008; **32**(2): 107–115. DOI: https://doi.org/10.1007/s10916-007-9113-9.

[20] Porwal P, et al. Indian Diabetic Retinopathy Image Dataset (IDRiD): A Database for Diabetic Retinopathy Screening Research. *Data*. 2018; **3**(3): 25. DOI: https://doi.org/10.3390/data3030025.

[21] Wilkinson CP, et al. Proposed International Clinical Diabetic Retinopathy and Diabetic Macular Edema Disease Severity Scales. *Ophthalmology*. 2003; **110**(9): 1677–1682. DOI: https://doi.org/10.1016/S0161-6420(03)00475-5.

[22] Mishra PK, et al. A Computational Modeling for the Detection of Diabetic Retinopathy Severity. *Bioinformation*. 2014; **10**(9): 556–561. DOI: https://doi.org/10.6026/97320630010556.

[23] Muztaba R, Malasan HL, and Djamal M. Development of an Automated Moon Observation System Using the ALTS-07 Robotic Telescope: 2. Progress Report on Standard Contrast Enhancement of Moon Crescent Image with OpenCV. *Journal of Physics: Conference Series*. 2022; **2214**: 012004. DOI: https://doi.org/10.1088/1742-6596/2214/1/012004.

[24] Hana FM and Maulida ID. Analysis of Contrast Limited Adaptive Histogram Equalization (CLAHE) Parameters on Finger Knuckle Print Identification. *Journal of Physics: Conference Series*. 2021; **1764**: 012049. DOI: https://doi.org/10.1088/1742-6596/1764/1/012049.

[25] Zhang P and Li F. A New Adaptive Weighted Mean Filter for Removing Salt-and-Pepper Noise. *IEEE Signal Processing Letters*. 2014; **21**(10): 1280–1283. DOI: https://doi.org/10.1109/LSP.2014.2333012.

[26] Faisal M, Wahono D, Purnomo IKE, Hariadi M, and Purnomo MH. Classification of Diabetic Retinopathy Patients Using Support Vector Machines (SVM) Based on Digital Retinal Image. *Journal of Theoretical and Applied Information Technology*. 2014; **59**(1): 197–204. Available from: http://www.jatit.org/volumes/Vol59No1/22Vol59No1.pdf.

[27] Raid AM, Khedr WM, El-dosuky MA, and Aoud M. Image Restoration Based on

Morphological Operations. *International Journal of Computer Science, Engineering and Information Technology (IJCSEIT)*. 2014; **4**(3): 9–21. DOI: https://doi.org/10.5121/ijcseit.2014.4302.

[28] Selvathi D, Parakash NB, and Balagopal N. Automated Detection of Diabetic Retinopathy for Early Diagnosis Using Feature Extraction and Support Vector Machine. *International Journal of Emerging Technology and Advanced Engineering*. 2012; **2**(11): 103–108.

[29] Zeng M, Li J, and Peng Z. The Design of Top-Hat Morphological Filter and Application to Infrared Target Detection. *Infrared Physics and Technology*. 2006; **48**(1): 67–76. DOI: https://doi.org/10.1016/j.infrared.2005.04.006.

[30] Miyamoto E and Jr. TM. *Fast Calculation of Haralick Texture Features*. Pittsburgh PA: Department of Electrical and Computer Engineering Carnegie Mellon University; 2005. Available from: http://users.ece.cmu.edu/~pueschel/teaching/18-799B-CMU-spring05/material/eizan-tad.pdf.

[31] Zulpe NS and Pawar VP. GLCM Textural Features for Brain Tumor Classification. *International Journal of Computer Science Issues*. 2012; **9**(3): 354–359. Available from: http://ijcsi.org/articles/Glcm-textural-features-for-brain-tumor-classification.php.

[32] Campbell C and Ying Y. Learning with Support Vector Machines. In C. Campbell and Y. Ying, *Synthesis Lectures on Artificial Intelligence and Machine Learning*. Switzerland: Springer Cham; 2011. DOI: https://doi.org/10.1007/978-3-031-01552-6.

[33] Ben-hur A and Weston J. A User's Guide to Support Vector Machines. In O. Carugo and F. Eisenhaber (eds), *Data Mining Techniques for the Life Sciences. Methods in Molecular Biology*, vol 609. New Jersey: Humana Press; 2010: 223–239. DOI: https://doi.org/10.1007/978-1-60327-241-4_13.

[34] Gayathri S, Krishna AK, Gopi VP, and Palanisamy P. Automated Binary and Multiclass Classification of Diabetic Retinopathy Using Haralick and Multiresolution Features. *IEEE Access*. 2020; **8**: 57497–57504. DOI: https://doi.org/10.1109/access.2020.2979753.

[35] Tharwat A. Classification Assessment Methods. *Applied Computing and Informatics*. 2018; **17**(1): 168–192. DOI: https://doi.org/10.1016/j.aci.2018.08.003.

[36] Rosadi MI, Sanjaya CB, and Hakim L. Klasifikasi Diabetic Retinopathy Menggunakan Seleksi Fitur Dan Support Vector Machine. *Jurnal RESISTOR (Rekayasa Sistem Komputer)*. 2018; **1**(2): 109–117. DOI: https://doi.org/10.31598/jurnalresistor.v1i2.312.

[37] Chen PN, et al. General Deep Learning Model for Detecting Diabetic Retinopathy. *BMC Bioinformatics*. 2021; **22**: 1–14. DOI: https://doi.org/10.1186/s12859-021-04005-x.

[38] Owhal MRR, Vaghasiya S, Tenkale A, and Pokale A. SVM for Diabetic Detection System. *International Journal of Scientific Research & Engineering Trends*. 2022; **8**(3): 1235–1237. Available from: https://ijsret.com/wp-content/uploads/2022/05/IJSRET_V8_issue3_325.pdf.

[39] Ranjan GSK, Verma AK, and Radhika S. K-Nearest Neighbors and Grid Search CV Based Real Time Fault Monitoring System for Industries. *2019 IEEE 5th International Conference for Convergence in Technology*; 2019: 9–13. DOI: https://doi.org/10.1109/I2CT45611.2019.9033691.

[40] Eagan B, Misfeldt M, and Siebert-Evenstone A. Advances in Quantitative Ethnography. *Proceedings of First Internasional Conference, ICQE 2019*; 2019. DOI: https://doi.org/10.1007/978-3-030-33232-7.

[41] Foster KR, Koprowski R, and Skufca JD. Machine Learning, Medical Diagnosis, and

Biomedical Engineering Research-Commentary. *BioMedical Engineering Online*. 2014; **13**(94): 1–9. DOI: https://doi.org/10.1186/1475-925X-13-94.

[42] Nasteski V. An Overview of the Supervised Machine Learning Methods. *Horizons*. 2017; **4**: 51–62. DOI: https://doi.org/10.20544/horizons.b.04.1.17.p05.

[43] Ruuska S, et al. Evaluation of the Confusion Matrix Method in the Validation of an Automated System for Measuring Feeding Behaviour of Cattle. *Behavioural Processes*. 2018; **148**: 56–62. DOI: https://doi.org/10.1016/j.beproc.2018.01.004.

[44] Seoud L, Chelbi J and Cheriet F. Automatic Grading of Diabetic Retinopathy on a Public Database. *Proceeding of Opthalmic Medical Image Analysis (OMIA) International Workshop*. 2015; **2**(2015): 97–104. DOI: https://doi.org/10.17077/omia.1032.